ACADEMIC
PRESS

Available online at www.sciencedirect.com
SCIENCE DIRECT®

Journal of Solid State Chemistry 171 (2003) 19–29

JOURNAL OF
SOLID STATE
CHEMISTRY

http://elsevier.com/locate/jssc

Nanostructured materials for advanced automotive de-pollution catalysts

Jan Kašpar* and Paolo Fornasiero

Dipartimento di Scienze Chimiche, University of Trieste, via L. Giorgieri 1, I- 34127 Trieste, Italy

Received 12 June 2002; received in revised form 1 September 2002; accepted 11 November 2002

Abstract

The present paper reviews the current understanding of CeO_2–ZrO_2 mixed oxides as promoters of the three-way catalysts. Emphasis is given on the role of the synthesis and it is shown that by adopting an appropriate design of the CeO_2–ZrO_2 system, nanostructured materials of high thermal stability can be prepared that are suitable for next generation automotive converters.

Keywords: Three-way catalysts; CeO_2–ZrO_2 solid solutions; CeO_2–ZrO_2 mixed oxides; Oxygen storage capacity; Nanostructured materials; CeO_2–ZrO_2–Al_2O_3 nanocomposites

---

1. Introduction

Catalytic abatement of toxic automotive exhaust represents one of the major applications of heterogeneous catalysts all over the world. In 1997, environmental catalysis accounted for 22% of $7.8 billion market sales of catalysts [1]. Nowadays, more than 95% of vehicles produced in the world are equipped with a catalytic converter, which, for the gasoline-fuelled engines, is almost exclusively based on the so-called three-way catalyst (TWC). TWCs are capable of simultaneously and efficiently converting CO, hydrocarbon (HC) and NO_x into harmless CO_2, H_2O and N_2, provided that the so-called air-to-fuel ratio (A/F) is constantly kept at the stoichiometry, i.e., under conditions where the amount of oxidants is equal to that of reducing agents. Since the advent of the TWCs, in the early 1980s, there has been a progressive tightening of the environmental legislation aimed at minimizing the amount of harmful pollutants emitted during the vehicle use [2]. For example, by the end of the 1960s, uncontrolled emissions of 40–60 g of CO/km were common to most of the passenger vehicles; this amount decreased to 2.3 g CO/km in 2000 and will be phased down to 1 g of CO/km in 2005 by European legislation (Euro phases 3 and 4). These limits represent reduction of, respectively, 94–96% and 97–98% compared to uncontrolled emissions. Recent US Tier 2 legislation, issued by EPA, challenged even more the catalyst/vehicle producers: besides the quite restrictive limits on the emissions, durability as high as 120,000 miles (about 180,000 km) will be phased-in by 2004 [3]. Clearly, in the last 20 years or so there has been a continuous evolution of TWCs technology, leading to more and more efficient TWCs [2,4].

However, the recent targets issued by EPA certainly represents a tough task making necessary the development of new materials with enhanced thermal stability. This is due to the fact that TWCs feature the so-called light-off type of conversion vs. temperature behavior, where the conversion steadily increases from 0% to 100%. The light-off temperature, conventionally taken as corresponding to 50% of conversion, is typically 513–623 K. As illustrated in Fig. 1, Californian ULEV threshold is typically overpassed within 30–40 s after the engine ignition. This means that to achieve the improvement of efficiency as required by the EU and US legislation, the catalyst heating time, i.e., time to reach light-off temperature, must be decreased down to 10–20 s. A cost-effective solution is to mount a secondary converter directly on the exhaust manifold

---

*Corresponding author. Fax: +39-040-5583903.
E-mail address: kaspar@units.it (J. Kašpar).

0022-4596/03/$ - see front matter © 2002 Elsevier Science (USA). All rights reserved.
doi:10.1016/S0022-4596(02)00141-X

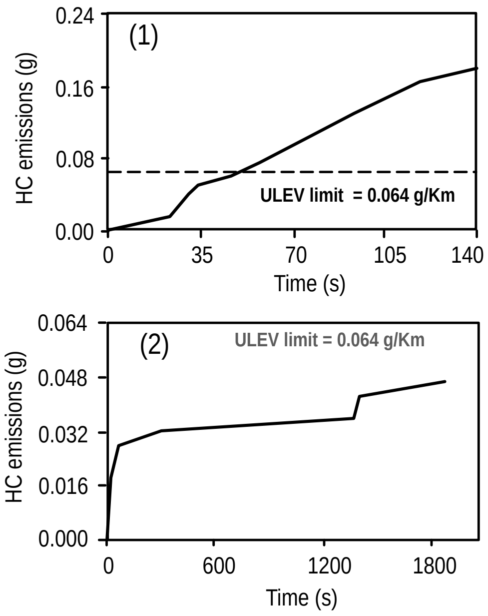

Fig. 1. Cumulative HC emissions measured immediately after a cold start of the engine during the federal test procedure (FTP cycle) performed on a US 1995 car: (1) engine-out emissions; (2) tailpipe emissions of the engine fitted with a close-coupled catalyst. Californian ULEV emission limits are indicated (adapted from [131]).

[5]. This, however, exposes the catalysts to extremely harsh conditions, where temperatures as high as 1373 K are reached.

Besides the noble metals (Pd and Pt to promote oxidation reaction and Rh to promote NO_x reduction), the current TWCs contain CeO_2–ZrO_2 mixed oxides as the so-called oxygen storage/release component. The oxygen storage capacity (OSC) is the ability of CeO_2-containing oxides to adsorb and release oxygen under, respectively, fuel-lean and fuel-rich conditions, according to the reaction

$$CeO_2 \underset{H_2O/CO_2}{\overset{H_2/CO}{\rightleftharpoons}} CeO_{2-x}.$$

The OSC is a crucial property of the TWCs since it helps to cope with the air-to-fuel oscillations and maintains a stoichiometric composition of the exhaust at the noble metal catalyst, necessary to attain the highest exhaust conversions. It is largely recognized that loss of the OSC property due to aging at high temperatures, which leads to sintering of the OSC component, is one of the major deactivation pathways for the TWCs. Thermal stabilization of the OSC component is therefore a major objective for developing advanced TWCs. The increasing use of ZrO_2- and CeO_2-based materials; not only as TWC promoters; but also in the field of ceramics, ionic conductors and as catalysts for industrial processes, grants rapid evolution to this field [6–8]. A CAS search for combination of CeO_2 and ZrO_2 as keywords, disclosed 171, 346 and 393 references in the years 1999–2001, respectively. Of these, 32% were patents. Despite this large amount of work, a fundamental comprehension of the relationships between the textural stability; redox properties and composition of the mixed oxide is still lacking. The aim of the present review is to critically focus the progress in the development of these materials showing how the design of the nanostructure may confer them new properties. The focus is given on the latest developments, since the earlier literature on the CeO_2–ZrO_2 has been covered previously [9].

2. Thermal stability and redox properties of CeO_2–ZrO_2 mixed oxides

2.1. Phase diagram and phase homogeneity

As described above, thermal stabilities up to 1373 K are required for future TWC applications. CeO_2–ZrO_2 mixed oxides are employed as the OSC component in modern TWCs, due to their excellent redox behavior and higher thermal stability compared to the traditionally employed CeO_2 [10–16]. Nowadays, there is a general agreement that the presence of a single-phase solid solution is preferable compared to microdomain — or phase-segregated non-homogeneous CeO_2–ZrO_2 mixed oxides, as the former systems generally lead to better textural stability and redox properties [9,16,18], even though some contradictory indications exist [17]. In addition to high activity and cost-effectiveness, durability is the most important property of a TWC; accordingly it is expected that a single-phase product should feature less modification during its lifetime in the converter. A question then arises: Why is there so wide research in the synthesis and characterization of these conceptually very simple mixed oxides? As shown in Eq. (1), ZrO_2 exists as a monoclinic phase at ambient pressure and below 1400 K. Tetragonal and cubic phases are formed at very high temperatures [19]:

$$\frac{\text{Monoclinic}}{P2_1/c} \overset{1400\,\text{K}}{\leftrightarrow} \frac{\text{Tetragonal}}{P4_2/nmc} \overset{2640\,\text{K}}{\leftrightarrow} \frac{\text{Cubic}}{Fm\bar{3}m}. \tag{1}$$

In contrast, CeO_2 crystallizes in the fluorite structure (space group $Fm\bar{3}m$). Given the relatively large difference (13%) between the cation radii of Ce^{4+} (0.097 nm) and Zr^{4+} (0.084 nm), a limited mutual solubility might be expected [20]. Consistently, only the t- and c-phase, found, respectively, at high (>80 mol%) and low (<20 mol%) ZrO_2 contents, are thermodynamically stable, while two metastable tetragonal phases (t', t'') were detected at intermediate compositions (Fig. 2) [21]. The exact location of the metastable boundary between the t' and t'' is still undefined and appears to depend on different parameters, particle size included [9,15].

The presence of metastable phases poses serious difficulties to researchers — sometimes underestimated

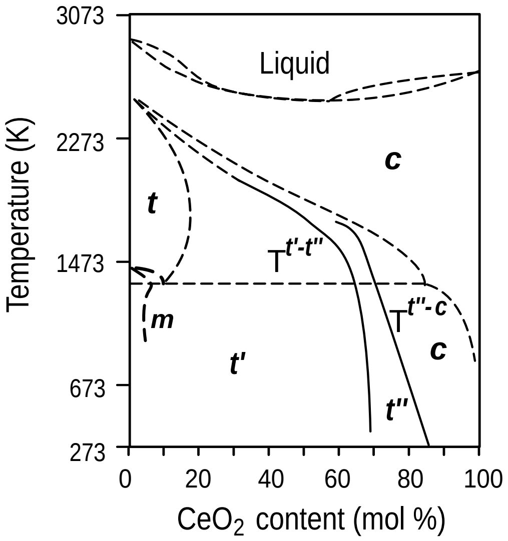

Fig. 2. CeO_2–ZrO_2 phase diagram: the metastable (t', t'') phase boundaries are included (adapted from [21]).

— when the homogeneity of the prepared mixed oxide has to be assessed. Vegards rule is typically applied to assess the presence of solid solution. Due to lower Zr^{4+} cation radius compared to Ce^{4+}, linear decreases of the cell parameter (or cell volume, when *t*-phases are included) is expected and, in fact, observed [22,23]. What are the difficulties when this criterion is applied to the nanosized CeO_2–ZrO_2 mixed oxides?

Generally speaking, the as-synthesized high-surface-area samples typically feature quite broad X-ray diffraction (XRD) peaks, due to the nanometric dimension of the crystallites. This makes difficult to obtain a reliable profile fitting of the XRD patterns using for example the Rietveld method, which, in our opinion, should be performed to properly assess the homogeneity of the mixed oxide. A partial sintering of the materials can be employed to improve the resolution of the XRD patterns, since an increase of the crystallite size makes the peaks sharp and minimizes the line broadening. After calcination at 1073–1273 K for 2–5 h, significant sharpening of the XRD patterns is indeed observed, which, however, sometimes led to the appearance of strongly asymmetric peaks in the XRD spectra [24,25]. This was generally attributed to formation of CeO_2- and ZrO_2-rich phases, which segregate upon calcination due to the metastable nature of the CeO_2–ZrO_2 system [24,25]. Other methods could, of course, be employed, such as Raman spectroscopy which easily detects non-incorporated CeO_2 and ZrO_2 [26], HREM [27], EXAFS [28], neutron diffraction [17], etc.; however, XRD is certainly one of the simplest and readily available techniques. We have investigated the problem of detection of single-phase CeO_2–ZrO_2 products to some extent [29,30] and observed that this observed phase segregation may often be related to the presence of compositional inhomogeneities generated by the synthesis method, rather than induced by calcination. As illustrated in Fig. 3 when calcination at 1273 K is performed on two $Ce_{0.5}Zr_{0.5}O_2$ samples for 5 h, no evidence of phase segregation (to the detection limit of the XRD technique) could be detected on the sample prepared by citrate synthesis, for which conditions were optimized to yield a single-phase product. On the contrary, the other sample showed clear indication of phase segregation into CeO_2- and ZrO_2-rich phases for the same calcination conditions. However, when the calcination time was increased to 100 h, even the sample prepared by the citrate route partially segregated [31]. Noticeably, both samples appeared as a single-phase

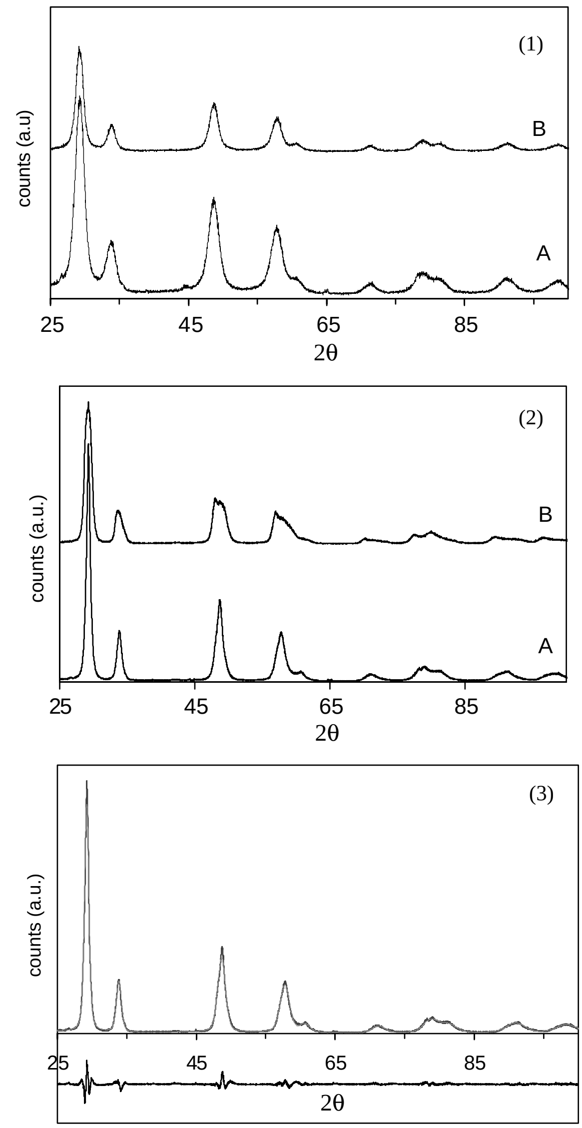

Fig. 3. Effects of calcination at 1273 K on two $Ce_{0.5}Zr_{0.5}O_2$ samples (A: ex-citrate, B: commercial) and Rietveld profile refinement of the XRD pattern of $Ce_{0.5}Zr_{0.5}O_2$ (sample A calcined for 5 h at 1273 K): (1) fresh samples, (2) calcined at 1273 K for 5 h, (3) Rietveld analysis (courtesy of Dr. Di Monte, University of Trieste) (adapted from [30,31]).

product when the XRD patterns of the fresh samples are considered. The interpretation of these data seems straightforward: the difference in the kinetics of phase segregation should be associated with a more homogeneously randomly distributed cation distribution being attained by the citrate synthesis. This result therefore provides a quick and easy criterion for the detection—to the level of sensitivity of this technique—of compositional in-homogeneities induced by an inadequate synthesis method.

2.2. Synthesis methodologies

An adequate synthesis methodology is a fundamental starting point for developing any new material. As emphasized above, for TWCs application the synthesis must confer to the CeO_2–ZrO_2-based materials the following properties:

- High thermal stability of the textural properties;
- Formation of a single-phase product;
- Suitable redox properties, the reduction at low temperatures being considered as a desirable property.

Last but not least, a cost-effective solution should be always considered for large-scale applications. As reported below, a great variety of methods have been investigated aiming at improving the above-quoted properties:

- solid-state synthesis [32,33]
- high-energy milling [34–37]
- coprecipitation
  - ○ room-temperature coprecipitation [11,12,14,25, 38–40]
  - ○ medium-to-high temperatures coprecipitation [41–46]
  - ○ surfactant-modified coprecipitation [47,48]
  - ○ ultrasound-induced coprecipitation [49]
- microemulsion precipitation [42,50–52]
- spray hydrolysis [53]
- combustion synthesis [42,52,54–58]
- electrochemical coprecipitation [59]
- chemical vapor deposition [60]
- sol–gel (like) synthesis
  - ○ alkoxide precursors [15,22,61,62]
  - ○ oxalic acid [23,63–65]
  - ○ citric acid [56,57,66–69]
  - ○ polyacrylic acid [42]
  - ○ hydrazine [70]
  - ○ poly-alcohols [56,57,71,72]
  - ○ urea [73]

As far as the solid-state synthesis and high-energy milling are concerned, these types of synthesis lead to preparation of ceramics, which, by the way, is a field where stabilized zirconias are largely employed [8]. Ceramic materials feature a high degree of densification and therefore sintering, which is exactly the opposite of what is the desirable property for catalytic applications; hence, these synthesis will not be further considered.

Due to the lack of a generally recognized criterion for detection of the homogeneity of the mixed oxide, a comparison of the different synthesis routes is not easy. In fact, the low calcination temperatures often employed to obtain a high-surface-area sample, do not allow unambiguous detection of a single-phase product as discussed above. Generally speaking, the sol–gel syntheses by controlled hydrolysis of alkoxide or similar precursors are considered to be a suitable method leading to high degree of homogeneity when mixed oxides are prepared. The underlying idea is that the preparation of the gel or gel-like precursor should lead to a homogeneous dispersion at molecular level of the Ce and Zr species, which then upon calcination lead to a intimately mixed oxide. However, it should be taken into account that when the rates of hydrolysis between the two metals are quite different, such as in the case of CeO_2 and ZrO_2 precursors, it may be quite difficult to simultaneously hydrolyze both precursors, particularly when $Zr(n\text{-}PrOH)_4$ is employed as a precursor. $Zr(n\text{-}PrOH)_4$ in fact rapidly reacts, even with air humidity, unless appropriate chemical modifications of the hydrolyzing process are adopted such as addition of acetylacetone which controls the rate of hydrolysis [74]. Even the choice of the solvent where the hydrolysis is performed, e.g. alcohols with different chain lengths, was shown to affect the nature of the product in the case of ZrO_2 [75]. In line with this consideration, application of the sol–gel methodology often led to detection of in-homogeneities, phase segregation, or presence of different phases even after relatively mild calcination as detected by the asymmetry of the diffraction peaks [15]. It should be noted, however, that when the experimental conditions of this process are optimized, the homogeneity of the mixed oxide can be improved [62].

A large number of preparations were performed by using organic complexing agents to generate a gel-like type of resins where homogeneous dispersion of the metal cations can, in principle, be achieved. Typically citric or oxalic acid, in the presence/absence of polyvinyl alcohol, are employed as complexing agents [56,64,68]. As shown earlier [76], rapid heating of the products obtained by this method leads to solids with appreciable surface area. More importantly, the fairly rapid transformation of the precursor into the final mixed oxide makes segregations in the oxide precursor unfavorable, which makes this synthesis method attractive for preparation of solid solutions. However, even in this case the choice of the experimental conditions is critical as the formation of the gel was affected even by the relative atmospheric humidity, that apparently modified the rates of formation of the sol and the gel [64,66]. The combustion synthesis [54] can be related to the citrate route in that also in this case an extremely rapid thermal decomposition of the "fuel-containing" solution of precursors is the key step conferring a homogeneous nature to the resulting product. There is another interesting aspect in this synthesis which is related to the fact that due to the high temperature experienced by the solid in the combustion, thermally stable products are in principle obtained. Thus, even complex oxides could be prepared by flame pyrolisis producing thermally stable materials with appreciable surface area [77].

The direct room-temperature precipitation methods also presents challenges as it appears difficult to find appropriate coprecipitation conditions for different CeO_2–ZrO_2 compositions even in the case of commercial products [16,78]. Thus, Hori et al. claimed that formation of homogenous solid solution can be attained by coprecipitation of Zr and Ce nitrates, however, when these samples were calcined at 1273 K for 2 h, significant phase segregation occurred [24], at variance with the results reported in Fig. 3. This was confirmed in a subsequent study where the presence of two phases was invariably detected when a coprecipitation method was employed [62]. Reverse precipitation method has also been employed for the preparation of CeO_2–ZrO_2 mixed oxides [79,80], apparently giving better phase homogeneity compared to the direct precipitation, even though some phase segregation was detected after calcination at 1273 K [80].

The recognition that fast quenching/precipitation may represent a key factor in producing homogeneous solid led to application of high-temperature hydrothermal synthesis methods. This methodology has long been applied to ZrO_2-containing coprecipitated products to increase the sample homogeneity and textural stability, also allowing to tune the crystal morphology/size, an important property for the preparation of high-performance ceramic materials [81–83]. Chuah et al. have investigated in detail the effects of conditions of hydrothermal treatment on the precipitated cakes, showing an important influence of these factors on the textural properties [84–87]. The rate of hydrolysis increases with temperature [88], which allows to "force" the hydrolysis and precipitation of the oxide even at relatively low temperature and acidic conditions [46]. Hirano and coworkers have investigated this kind of synthesis in detail showing that ultrafine CeO_2-containing particles may be effectively prepared [41,89,90] and these products can feature quite remarkably high surface area even after heat treatment at 1273 K [46]. At very high—near water critical—temperatures, the rate of hydrolysis becomes extremely rapid, which allowed to develop a continuous flow-through reactor to efficiently produce mixed oxides with various compositions and different particle morphology, according to the reaction temperature and feeding conditions [91]. Recently, this technique has been extended to the preparation of CeO_2–ZrO_2 mixed oxides as well [43,92].

In summary, there are a number of issues concerning the preparation of these apparently simple oxides, however, by appropriately designing the synthesis conditions and methodology, homogeneous nanodispersed CeO_2–ZrO_2 solid solutions have been successfully obtained.

For TWC application, however, besides the homogeneity of the mixed oxide, textural stability is fairly important. Even though early studies showed that due to the strong modification of the oxygen sublattice [93], redox processes can occur in the bulk of these oxides at low temperatures even when sintered at 1873 K [94,95], the stability of the surface area is an important issue. A comparison of CO and H_2 as reducing agents under dynamic conditions, clearly revealed that for the latter, the OSC occurs at the surface via a spillover mechanism at room temperature in the presence of reduced noble metal, whilst the reduction occurs deep into the bulk at temperatures as low as 373–473 K [96]. In contrast, when CO is employed as the reducing agent, the redox processes occur at higher temperatures, but, most important, the extent of CO-OSC is related to the surface area of the CeO_2–ZrO_2 mixed oxide, surface reactions being the rate-limiting processes in this case [24,96,97]. A non-exhaustive survey of surface BET areas obtained for different CeO_2–ZrO_2 mixed oxides prepared by different synthesis routes is reported in Table 1. Care should be taken when such comparison is made due to the different synthesis conditions employed among the various researchers, however, the effect of insertion of ZrO_2 into the CeO_2 lattice is clearly confirmed also by these recent data gathered from the literature, high ZrO_2 content favoring highest textural stability under equivalent synthesis conditions. This can be related to a retarding effect of ZrO_2 insertion into the CeO_2 lattice on the rate of sintering of the oxide [98]. Another observation is that the use of a sol–gel route resulted in a better textural stability compared to the coprecipitation technique for a $Ce_{0.9}Zr_{0.1}O_2$ (Table 1), which can be related to a better phase homogeneity achieved by the former synthesis method [18]. This result again stresses the necessity of designing an appropriate synthesis strategy to achieve a homogeneous solid solution as a product.

With the aim of addressing the issue of surface area, preparation of mesoporous solids by addition of surfactants in the synthesis has been attempted by some authors [48,99–102]. At variance with ZrO_2-based materials where assessed synthesis methodologies to produce mesoporous materials have been developed [103], these attempts to produce such ordered

Table 1
Effect of calcination temperature and time on BET surface areas of CeO_2 and CeO_2–ZrO_2 mixed oxides

Composition	Synthesis method	Calcination conditions and BET surface area				Refs./notes
		Temp./time	BET area	Temp./time	BET Area	
CeO_2	Co-precpt.	823 K/2 h	55	973 K/2 h	5	[79]
$Ce_{0.8}Zr_{0.2}O_2$	Co-precpt.	823 K/2 h	85	973 K/2 h	30	[79]
$Ce_{0.83}Zr_{0.17}O_2$	Co-precpt.	773 K/6 h	85	973 K/6 h	58	[80]/3 $m^2 g^{-1}$ (1273 K, 6 h)
$Ce_{0.67}Zr_{0.33}O_2$	Co-precpt.	773 K/6 h	104	973 K/6 h	70	[80]/8 $m^2 g^{-1}$ (1273 K, 6 h)
$Ce_{0.90}Zr_{0.10}O_2$	Co-precpt.	1053 K/4 h	25	1173 K/4 h	18	[62]
	Sol–gel	1053 K/4 h	56	1173 K/4 h	35	[62]
$Ce_{0.75}Zr_{0.25}O_2$	Co-precpt.	773 K/1 h	72	1273 K/4 h	14	[24]
$Ce_{0.83}Zr_{0.17}O_2$	Co-precpt.	773 K/1 h	87	1273 K/4 h	14	[24]
$Ce_{0.5}Zr_{0.5}O_2$	Co-precpt. at 573 K	573 K	105	1273 K/1 h	15	[92]
$Ce_{0.2}Zr_{0.8}O_2$	Co-precpt. at 373 K			1273 K/	50	[46]
$Ce_{0.6}Zr_{0.4}O_2$	Co-precpt. at 373 K			1273 K/	43	[46]
$Ce_{0.8}Zr_{0.2}O_2$	Co-precpt. at 373 K			1273 K/	33	[46]
$Ce_{0.8}Zr_{0.2}O_2$	Co-precpt./organic template	723 K/2 h	209	1173 K/2 h	56	[47]
$Ce_{0.5}Zr_{0.5}O_2$	Cellulose template	1073 K/2 h	129	1323 K/12 h	30	[104]

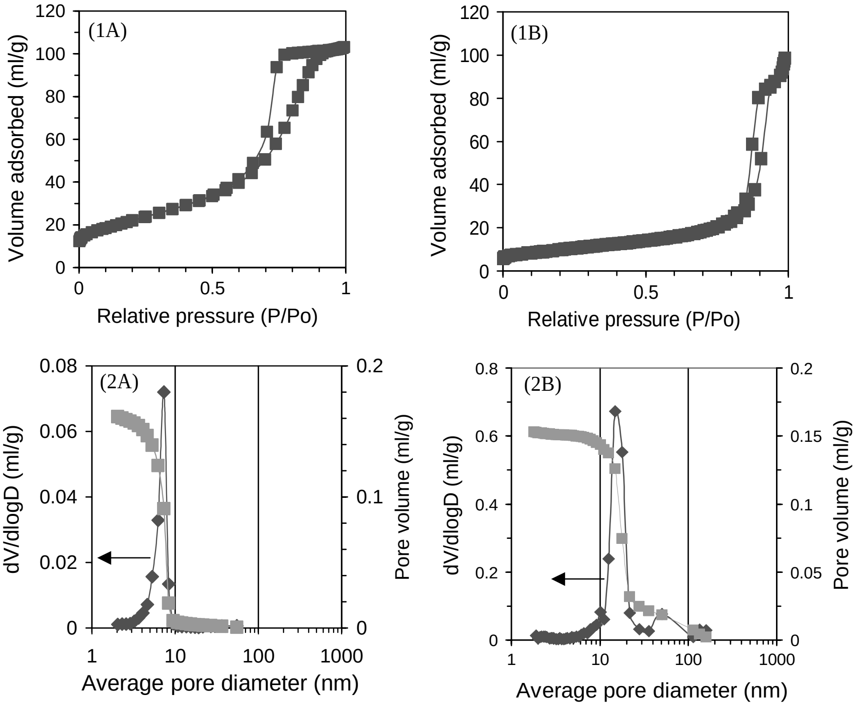

Fig. 4. N_2 adsorption isotherm (1) and cumulative pore volume and pore distribution (2) as detected from N_2 desorption isotherm using the BJH method on two samples (A and B) single-phase $Ce_{0.2}Zr_{0.8}O_2$ solid solution [110] (courtesy of MEL Chemical, Manchester, UK).

CeO_2–ZrO_2 mesoporous systems were partly successful [48]. Materials with high surface area (200–300 $m^2 g^{-1}$) could, in fact, be prepared, however, when the calcination temperature was increased above 1073 K, strong decline of BET surface area was observed [47]. In fact, despite the high surface area of these products, comparable sintering rates were observed in samples either conventionally coprecipitated and coprecipitated by a template-assisted route [9].

An interesting exception is the use of cellulose as templating agent, recently reported by researchers from Ford Motor Co. [104] that showed that by adsorbing the precursors on the surface of different kind of papers, the morphology of the obtained product closely follows that of the starting cellulose-containing material. Thus, filamentous particles of CeO_2–ZrO_2 mixed oxides were observed by SEM that closely resembled the morphology of the starting cellulose. Such morphology of the particles adversely affected the sintering process, allowing BET surface areas as high as 30 $m^2 g^{-1}$ after calcination at 1323 K to be obtained.

These data clearly reveal that the design of the pore structure also plays a key role in enhancing the thermal stability of the CeO_2–ZrO_2 materials. The importance of this aspect is clearly exemplified in Fig. 4, where the pore distribution is shown for two samples of single-phase $Ce_{0.2}Zr_{0.8}O_2$ products, as checked by Rietveld analysis after calcination at 1273 K. Both samples were prepared to feature comparable BET areas (sample A: $27\,m^2\,g^{-1}$ and B: $35\,m^2\,g^{-1}$), however, sample B was purposely synthesized in such a way to feature a pore distribution centered at pore radii significantly higher compared to sample A. When these samples were calcined at 1273 K for 5 h, the surface area of sample A collapsed to $4\,m^2\,g^{-1}$, whilst an appreciable value of $22\,m^2\,g^{-1}$ was measured over sample B. This accounts for a relative decrease of surface area of 85% and 37%, respectively, for samples A and B. In terms of durability of the TWCs, clearly the behavior observed for sample B is more desirable because such relatively small drop of surface area after calcination at 1273 K suggests that negligible loss of precious metal due to metal particle encapsulation should occur in this case. Metal particle encapsulation upon aging at high temperatures was indeed shown to be an important pathway leading to deactivation of the model CeO_2–ZrO_2 containing TWCs [105,106]. Last but not least, the investigation of the reduction behavior and dynamic-OSC, using both CO and H_2 as reducing agents disclosed remarkably different behaviors between the two samples, as exemplified in Fig. 5 where the effects of severe and mild oxidation pre-treatments of the TPR profile are reported. Previous works have shown that reduction behavior of CeO_2–ZrO_2 is strongly affected by the temperature of the pre-oxidation performed before the TPR run: a mild oxidation generates a low-temperature reduction profile whereas the severe-high-temperature oxidation generates a high-temperature reduction profile, both the reduction phenomena being reversibly inter-converted [13,107,108]. The reduction behavior of sample A, shown in Fig. 5, illustrates this kind of modifiable reduction behavior. The exact origin of this sensitivity to the pre-treatment is still unclear even if the sintering of the mixed oxides leading to surface cerium enrichment was recently indicated as a pre-requisite to obtain this kind of variable reduction behavior [109]. In agreement with this observation, the texturally stable sample B features an almost constant—pre-treatment independent—reduction behavior (Fig. 5). More importantly, sample B showed significantly better performances under the dynamic OSC conditions, i.e., conditions that are closer to the real exhaust conditions than a TPR run, compared to sample A [110]. This confirms an important role of the textural stability on the redox properties, in addition to those structural [95].

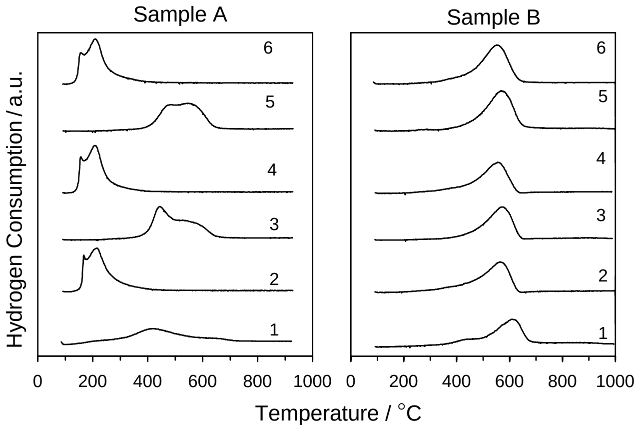

Fig. 5. Temperature-programmed reduction profiles of single-phase $Ce_{0.2}Zr_{0.8}O_2$ samples with different textural properties (samples A and B from Fig. 4, calcined at 1273 K for 5 h): effects of pre-treatments/redox aging. A severe oxidation at 1173 K (SO) precedes third and fifth TPR profiles, while mild oxidation at 700 K precedes all the other TPR runs (adapted from [110]).

3. Effect of addition of Al_2O_3 to CeO_2–ZrO_2 mixed oxides

Given the importance of the textural stability for practical application of the CeO_2–ZrO_2 in the TWCs, the design of nanocomposites where the CeO_2–ZrO_2 phase is dispersed over a stable inert support could represent a suitable way to improve thermal stability of these systems. To date, relatively few papers have been devoted to this topic and only recently the effects of addition of Al_2O_3 on the thermal stability and reduction behavior of CeO_2–ZrO_2 mixed oxides have been reported [29,111–122]. There are some reasons that could account for the lack of extensive studies in this area. As observed above, the synthesis of the single-phase CeO_2–ZrO_2 may be difficult, requiring appropriate synthesis strategies to be adopted. This clearly becomes even more important when a third component (Al_2O_3) is added. Another important aspect is that while nanodispersed CeO_2 particles could be obtained by impregnating Al_2O_3 with a $Ce(NO_3)_3$ precursor and subsequent calcination [123], this does not necessarily result in a good OSC promoter. As shown by detailed studies reported more than a decade ago, the intimate contact between Al_2O_3 and the highly dispersed CeO_2 particles, which is generated by the deposition process, favors formation of $CeAlO_3$ after high-temperature aging that deactivates the OSC component [124,125]. These previous observations and also patent claims (see for example US patent 5,945,369, issued on August 31, 1999) therefore clearly indicated the unsuitability of impregnation of CeO_2 on Al_2O_3 for production of effective OSC systems. Accordingly, it is usual practice to employ pre-formed CeO_2 or CeO_2–ZrO_2 particles to make the TWCs. These particles are then suspended with Al_2O_3 and the other components, and finally wash-coated on the honeycomb.

Let us, however, consider the effect of Al_2O_3 addition to CeO_2–ZrO_2 mixed oxides. As in the case of unsupported mixed oxides, optimized synthesis procedures are needed to produce single-phase CeO_2–ZrO_2 products at the surface of Al_2O_3 [9]. The above-suggested criterion for detection of single-phase products can be conveniently employed also for Al_2O_3-supported products [29].

A perusal of the data reported in the literature shows that simple impregnation of Al_2O_3 with nitrates of ceria and zirconia is ineffective in producing homogeneous products, which apparently is due to the fact that ZrO_2 tends to spread as an amorphous layer over the surface of Al_2O_3 [111,126]. Use of a complexing agent (citric acid) [115] or a microemulsion co-precipitation [127] is necessary to obtain a reasonably good phase homogeneity of the mixed oxide, even though when the CeO_2–ZrO_2 content is increased from 10 to 33 wt%, some of the ZrO_2 tends to segregate on the Al_2O_3 surface [127]. These difficulties are obviously higher at intermediate CeO_2–ZrO_2 compositions, where the opportunity for compositional inhomogeneities is statistically higher [111]. It should be noted that the use of the latter deposition technique generates fairly dispersed CeO_2–ZrO_2 particles at Al_2O_3 surface; average particle diameter of 2–3 nm was indeed detected both for 10 and 33 wt% loading of the mixed oxide [127].

The most important effect of the deposition of CeO_2–ZrO_2 on Al_2O_3 is certainly the increase of the thermal stability of the CeO_2–ZrO_2 mixed oxide compared to the unsupported one. Whereas single-phase XRD pattern such the one as shown in Fig. 3 could be detected for a $Ce_{0.6}Zr_{0.4}O_2$ solid solution for relatively short calcination temperatures, the presence of a single-phase solid solution was detected even after 100 h of calcination at 1273 K for a $Ce_{0.6}Zr_{0.4}O_2/Al_2O_3$ nanocomposite [29]. This could be attributed either to a synergic stabilization between the Al_2O_3 and CeO_2–ZrO_2 phases or to the retarding effect of the Al_2O_3 on the sintering rate of the supported CeO_2–ZrO_2 phase. A particle size of 6 nm was in fact detected after such harsh calcination, which is far below the critical size of 15–20 nm that was suggested as a limiting value above which the mixed oxide tends to segregate [27]. For comparison, particles as large as 20 nm are easily detected after 5 h of calcination at 1273 K in the absence of Al_2O_3. This result clearly illustrates the importance of nanostructuring the composite oxide, since the citrate route employed in the deposition, leads to highly sinterable materials in the case of the unsupported CeO_2–ZrO_2 solid solutions. However, this stabilization effect of Al_2O_3 addition on the phase stability of CeO_2–ZrO_2 solution of intermediate composition appears to be limited up to 1273 K, since beginning of phase segregation was clearly detected when the calcination temperature was increased to 1373 K [115]. At such high temperature, the issue of the CeO_2–ZrO_2 composition has to be considered: consistent with the unsupported CeO_2–ZrO_2 samples, ZrO_2-rich composition appeared more thermally stable leading to materials that featured appreciably stable dynamic-OSC and single-phase $Ce_{0.2}Zr_{0.8}O_2$ solid solution even after calcination at 1373 K for 24 h [115].

Of less importance, but still interesting is the fact that the stabilization of CeO_2–ZrO_2/Al_2O_3 is synergic in that the presence of the supported CeO_2–ZrO_2 hinders the transformation of the transitional (γ and δ) Al_2O_3 into the α-Al_2O_3. This could be related to the fact, that in analogy to what is observed for CeO_2 [123], the CeO_2–ZrO_2 tends to grow as flat two dimensional patches, which prevail over the three-dimensional ones at lower CeO_2–ZrO_2 loadings [127]. The stabilization of Al_2O_3 is also observed when either ZrO_2 [126] or CeO_2 [128] are supported on Al_2O_3, CeO_2 being particularly effective under reducing conditions due to formation of $CeAlO_3$.

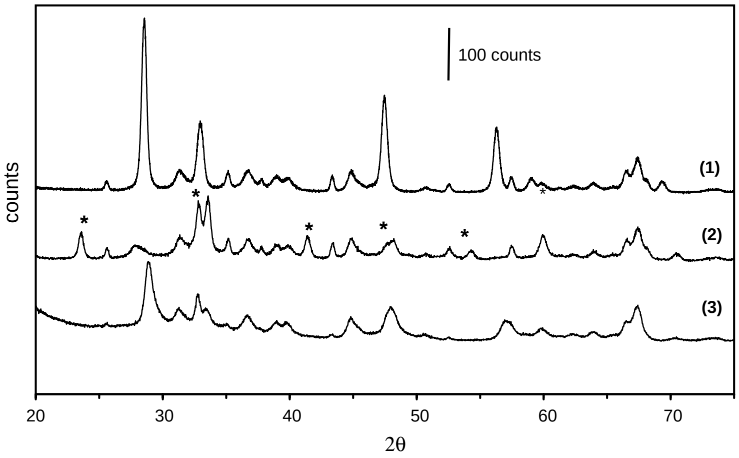

Fig. 6. Powder XRD profiles of (1) CeO_2/Al_2O_3 calcined at 1273 K for 5 h, (2) CeO_2/Al_2O_3 calcined at 1273 K for 5 h, subjected to a TPR up to 1273 K followed by an oxidation at 700 K, and (3) $Ce_{0.6}Zr_{0.4}O_2/Al_2O_3$ calcined at 1273 K for 5 h, subjected to a TPR up to 1273 K followed by an oxidation at 700 K. (*) peaks belonging to $CeAlO_3$ (adapted from [116]).

Concerning the mutual interaction between the CeO_2-containing moiety and Al_2O_3, the addition of ZrO_2 plays a fundamental role in terms of oxygen storage. As commented above, dispersion of CeO_2 over Al_2O_3 and its reduction at high temperatures leads to formation of $CeAlO_3$ that cannot be easily re-oxidized [114,124,125,129]. When ZrO_2 is added in the form of solid solution, this deactivation pattern is strongly suppressed as shown in Fig. 6: in contrast to CeO_2/Al_2O_3, $CeAlO_3$ could not be detected by XRD technique when ZrO_2 was incorporated into the nanocomposite mixed oxide.

While the stabilization effect of Al_2O_3 addition on the OSC properties of CeO_2–ZrO_2 mixed oxides appears well established, the effects on catalytic performances of precious metal containing catalysts are less clear. A recent study of effects of engine exhaust aging at 1273 K on catalytic performances of a $Pd/Ce_{0.5}Zr_{0.5}O_2/Al_2O_3$ catalyst disclosed that such an aging procedure led to the loss of the beneficial effect of the CeO_2–ZrO_2 mixed oxide on the activity of the catalyst [120].

4. Conclusions

The review of the recent progresses in the field of CeO_2–ZrO_2-based oxygen storage promoters for advanced TWC applications clearly revealed the crucial importance of an appropriate synthesis strategy to confer desirable redox properties and textural stability to these mixed oxides. The design of the mixed oxide must be performed at a subtle and intimate level because even differences in the mesoporosity may affect the redox properties at "equal" composition and phase purity.

Addition of Al_2O_3 to the CeO_2–ZrO_2 mixed oxides has been demonstrated to be a formidable tool that produces nanocomposite materials with thermal stabilities up to 1373 K, despite use of conventional synthesis strategies. This evidences the necessity of developing and applying new synthesis strategies to design even more effective materials suitable for the next generation TWCs and other thermally demanding applications such as catalytic combustion. For example, by nanostructuring CeO_2-containining hexaaluminates via a reverse microemulsion synthesis, thermal stabilities up to 1573 K could be achieved [130].

Acknowledgments

The authors gratefully thank their colleagues Drs. R. Di Monte, N. Hickey, and Prof. M. Graziani, University of Trieste, and Drs. P. Moles and C. Norman from MEL Chemicals for their valuable contribution to the development of the chemistry of CeO_2–ZrO_2 mixed oxides and helpful discussions. MEL Chemicals, University of Trieste, Fondo Trieste 1999, CNR Rome, MURST-PRIN 2000 "Catalysis for the reduction of the environmental impact of mobile source emissions", and project "Urban Atmosphere"—Consortium INCA are gratefully acknowledged for financial support.

References

[1] M. McCoy, Chem. Eng. News 77 (1999) 17.
[2] M. Shelef, R.W. McCabe, Catal. Today 62 (2000) 35.
[3] Environmental Protection Agency, Fed. Regist. 65 (2000) 6697.
[4] R.M. Heck, R.J. Farrauto, Catalytic Air Pollution Control. CommercialTechnology, Van Nostrand Reinhold, New York, 1995, pp. 1.
[5] R.J. Farrauto, R.M. Heck, Catal. Today 51 (1999) 351.
[6] H.L. Tuller, Solid State Ionics. 131 (2000) 143.
[7] S. Bernal, J. Kaspar, A. Trovarelli, Recent progress in catalysis by ceria and related compounds, S.Bernal, J. Kaspar, A. Trovarelli (Eds.), Catal. Today 50 (1999) Vol. 2, Elsevier Science, Amsterdam, 1999, pp. 173–443.
[8] A. Trovarelli, in: A. Trovarelli (Ed.), Catalysis by Ceria and Related Materials, Vol. 2, Imperial College Press, London, 2002, pp. 1–500.
[9] J. Kaspar, P. Fornasiero, M. Graziani, Catal. Today 50 (1999) 285.
[10] S. Matsumoto, N. Miyoshi, M. Kimura, M. Ozawa, A. Isogai,Toyota Motor Corp., Toyota Central Research and Development Laboratories, I. Assignees. DE 3737419 (Issued: 1988 May 19), Priority: DE 3737419 871104.
[11] M. Ozawa, M. Kimura, A. Isogai, J. Alloys Compd. 193 (1993) 73.
[12] T. Murota, T. Hasegawa, S. Aozasa, H. Matsui, M. Motoyama, J. Alloys Compd. 193 (1993) 298.
[13] G. Balducci, P. Fornasiero, R. Di Monte, J. Kaspar, S. Meriani, M. Graziani, Catal. Lett. 33 (1995) 193.
[14] F. Zamar, A. Trovarelli, C. de Leitenburg, G. Dolcetti, J. Chem. Soc. Chem. Commun. (1995) 965.
[15] P. Fornasiero, G. Balducci, R. Di Monte, J. Kaspar, V. Sergo, G. Gubitosa, A. Ferrero, M. Graziani, J. Catal. 164 (1996) 173.
[16] J.P. Cuif, G. Blanchard, O. Touret, A. Seigneurin, M. Marczi, E. Quémeré, SAE, 961906, 1996.
[17] T. Egami, W. Dmowski, R. Brezny, SAE, 970461, 1997.
[18] Y. Sun, P.A. Sermon, J. Mater. Chem. 6 (1996) 1025.
[19] M. Yashima, M. Kakihana, M. Yoshimura, Solid State Ionics. 86-8 (1996) 1131.
[20] A.R. West, Basic Solid State Chemistry, 2nd. Edition, Wiley, Chichester, 1999, pp. 1–480.
[21] M. Yashima, H. Arashi, M. Kakihana, M. Yoshimura, J. Am. Ceram. Soc. 77 (1994) 1067.
[22] C.K. Narula, L.P. Haack, W. Chun, H.W. Jen, G.W. Graham, J. Phys. Chem. B. 103 (1999) 3634.
[23] K. Otsuka, Y. Wang, M. Nakamura, Appl. Catal. A. Gen. 183 (1999) 317.
[24] C.E. Hori, H. Permana, K.Y.S. Ng, A. Brenner, K. More, K.M. Rahmoeller, D.N. Belton, Appl. Catal. B Environ. 16 (1998) 105.
[25] C. Bozo, F. Gaillard, N. Guilhaume, Appl. Catal. A Gen. 220 (2001) 69.
[26] G. Colon, M. Pijolat, F. Valdivieso, H. Vidal, J. Kaspar, E. Finocchio, M. Daturi, C. Binet, J.C. Lavalley, R.T. Baker, S. Bernal, J. Chem. Soc. Faraday Trans. 94 (1998) 3717.
[27] G. Colon, F. Valdivieso, M. Pijolat, R.T. Baker, J.J. Calvino, S. Bernal, Catal. Today 50 (1999) 271.

[28] G. Vlaic, R. Di Monte, P. Fornasiero, E. Fonda, J. Kaspar, M. Graziani, J. Catal. 182 (1999) 378.

[29] R. Di Monte, P. Fornasiero, J. Kaspar, P. Rumori, G. Gubitosa, M. Graziani, Appl. Catal. B Environ. 24 (2000) 157.

[30] P. Fornasiero, R. Di Monte, J. Kaspar, T. Montini, M. Graziani, Stud. Surf. Sci. Catal. 130 (2000) 1355.

[31] J. Kaspar, P. Fornasiero, Structural properties and thermal stability of ceria-zirconia and related materials, in: A. Trovarelli (Ed.), Catalysis by Ceria and Related Materials, Imperial College Press, London, 2002, pp. 217–241. (Chapter 6)

[32] A.I. Leonov, A.B. Andreeva, E.K. Keler, Izv. Akad. Nauk SSSR Neorg. Mater. 2 (1966) 137.

[33] K. Eguchi, N. Akasaka, H. Mitsuyasu, Y. Nonaka, Solid State Ionics 135 (2000) 589.

[34] Y.L. Chen, M. Qi, D.Z. Yang, K.H. Wu, Mater. Sci. Eng. A-Struct. Mater. 183 (1994) L9.

[35] C. de Leitenburg, A. Trovarelli, F. Zamar, S. Maschio, G. Dolcetti, J. Llorca, J. Chem. Soc. Chem. Commun. (1995) 2181.

[36] F. Zamar, A. Trovarelli, C. de Leitenburg, G. Dolcetti, Stud. Surf. Sci. Catal. 101 (1996) 1283.

[37] A. Suda, H. Sobukawa, T. Suzuki, T. Kandori, Y. Ukyo, M. Sugiura, J. Ceram. Soc. Jpn. 109 (2001) 177.

[38] M.Y. Sinev, G.W. Graham, L.P. Haack, M. Shelef, J. Mater. Res. 11 (1996) 1960.

[39] O.A. Kirichenko, G.W. Graham, W. Chun, R.W. McCabe, Stud. Surf. Sci. Catal. 118 (1998) 411.

[40] C.E. Hori, A. Brenner, K.Y.S. Ng, K.M. Rahmoeller, D. Belton, Catal. Today 50 (1999) 299.

[41] M. Hirano, E. Kato, J. Ceramic. Soc. Jpn. 104 (1996) 958.

[42] A.P. Oliveira, M.L. Torem, Powder Technol. 119 (2001) 181.

[43] A. Cabanas, J.A. Darr, E. Lester, M. Poliakoff, Chem. Commun. (2000) 901.

[44] R.R. Piticescu, C. Bogdanescu, T. Segarceanu, T. Velea, Int. J. Mater. Prod. Technol. 15 (2000) 252.

[45] M. Hirano, T. Miwa, M. Inagaki, J. Ceram. Soc. Jpn. 109 (2001) 401.

[46] M. Hirano, T. Miwa, M. Inagaki, J. Solid State Chem. 158 (2001) 112.

[47] D. Terribile, A. Trovarelli, J. Llorca, C. de Leitenburg, G. Dolcetti, Catal. Today 43 (1998) 79.

[48] M.P. Kapoor, A. Raj, Y. Matsumura, Microporous Mesoporous Mat. 44 (2001) 565.

[49] L.X. Yin, Y.Q. Wang, G.S. Pang, Y. Koltypin, A. Gedanken, J. Colloid Interface Sci. 246 (2002) 78.

[50] T. Masui, K. Fujiwara, Y.M. Peng, T. Sakata, K. Machida, H. Mori, G. Adachi, J. Alloys Compd. 269 (1998) 116.

[51] A. Martinez Arias, M. Fernandez Garcia, V. Ballesteros, L.N. Salamanca, J.C. Conesa, C. Otero, J. Soria, Langmuir 15 (1999) 4796.

[52] K. Takatori, T. Tani, N. Watanabe, N. Kamiya, J. Nanopart. Res. 1 (1999) 197.

[53] E. Djurado, E. Meunier, J. Solid State Chem. 141 (1998) 191.

[54] S.T. Aruna, K.C. Patil, Nanostruct. Mater. 10 (1998) 955.

[55] E. Zhou, S. Bhaduri, S.B. Bhaduri, I.R. Lewis, P.R. Griffiths, Int. J. Self-Propag. High-Temp. Synth. 7 (1998) 317.

[56] A.L. Quinelato, E. Longo, E.R. Leite, M.I.B. Bernardi, J.A. Varela, J. Mater. Sci. 36 (2001) 3825.

[57] A.L. Quinelato, E. Longo, E.R. Leite, J.A. Varela, Appl. Organomet. Chem. 13 (1999) 501.

[58] D.G. Lamas, R.E. Juarez, G.E. Lascalea, N.E. Walsoe de Reca, J. Mater. Sci. Lett. 20 (2001) 1447.

[59] A. Mukherjee, D. Harrison, E.J. Podlaha, Electrochem. Solid. State. Lett. 4 (2001) D5.

[60] D. Barreca, G.A. Battiston, U. Casellato, R. Gerbasi, E. Roncari, E. Tondello, P. Zanella, J. Phys. IV 11 (2001) 453.

[61] S. Rossignol, Y. Madier, D. Duprez, Catal. Today 50 (1999) 261.

[62] S. Rossignol, F. Gerard, D. Duprez, J. Mater. Chem. 9 (1999) 1615.

[63] T. Masui, Y.M. Peng, K. Machida, G. Adachi, Chem. Mater. 10 (1998) 4005.

[64] T. Settu, R. Gobinathan, J. Eur. Ceram. Soc. 16 (1996) 1309.

[65] K. Higashi, K. Sonoda, H. Ono, S. Sameshima, Y. Hirata, J. Mater. Res. 14 (1999) 957.

[66] P.V. Ananthapadmanabhan, N. Venkatramani, V.K. Rohatgi, A.C. Momin, K.S. Venkateswarlu, J. Eur. Ceram. Soc. 6 (1990) 111.

[67] A.L. Quinelato, E. Longo, L.A. Perazolli, J.A. Varela, J. Eur. Ceram. Soc. 20 (2000) 1077.

[68] P. Vidmar, P. Fornasiero, J. Kaspar, G. Gubitosa, M. Graziani, J. Catal. 171 (1997) 160.

[69] M. Kakihana, S. Kato, M. Yashima, M. Yoshimura, J. Alloys Compd. 280 (1998) 125.

[70] S. Hirano, A. Kawabata, M. Yoshinaka, K. Hirota, O. Yamaguchi, J. Am. Ceram. Soc. 78 (1995) 1414.

[71] M. Inoue, K. Sato, T. Nakamura, T. Inui, Catal. Lett. 65 (2000) 79.

[72] S. Yamamoto, M. Kakihana, S. Kato, J. Alloys Comp. 297 (2000) 81.

[73] M. Thammachart, V. Meeyoo, T. Risksomboon, S. Osuwan, Catal. Today 68 (2001) 53.

[74] M. Chatry, M. Henry, J. Livage, Mater. Res. Bull. 29 (1994) 517.

[75] M.C. Caracoche, P.C. Rivas, M.M. Cervera, R. Caruso, E. Benavidez, O. deSanctis, M.E. Escobar, J. Am. Ceram. Soc. 83 (2000) 377.

[76] C. Marcilly, P. Courty, B. Delmon, J. Am. Ceram. Soc. 53 (1970) 56.

[77] R. Leanza, I. Rossetti, L. Fabbrini, C. Oliva, L. Forni, Appl. Catal. B Environ. 28 (2000) 55.

[78] J.P. Cuif, G. Blanchard, O. Touret, A. Seigneurin, M. Marczi, E. Quémeré, SAE, 970463, 1997.

[79] C. de Leitenburg, A. Trovarelli, J. Llorca, F. Cavani, G. Bini, Appl. Catal. A Gen. 139 (1996) 161.

[80] C. Bozo, N. Guilhaume, E. Garbowski, M. Primet, Catal. Today 59 (2000) 33.

[81] E. Tani, M. Yoshimura, S. Somiya, J. Am. Ceram. Soc. 66 (1983) 11.

[82] Y. Hakuta, S. Onai, H. Terayama, T. Adschiri, K. Arai, J. Mater. Sci. Lett. 17 (1998) 1211.

[83] S. Somiya, T. Akiba, J. Eur. Ceram. Soc. 19 (1999) 81.

[84] K.S. Chan, G.K. Chuah, S. Jaenicke, J. Mater. Sci. Lett. 13 (1994) 1579.

[85] G.K. Chuah, S. Jaenicke, S.A. Cheong, K.S. Chan, Appl. Catal. A Gen. 145 (1996) 267.

[86] G.K. Chuah, S. Jaenicke, Appl. Catal. A Gen. 163 (1997) 261.

[87] G.K. Chuah, S. Jaenicke, B.K. Pong, J. Catal. 175 (1998) 80.

[88] A. Rabenau, Angew. Chem. Int. Ed. 24 (1985) 1026.

[89] M. Hirano, E. Kato, J. Am. Ceram. Soc. 79 (1996) 777.

[90] M. Hirano, E. Kato, J. Am. Ceram. Soc. 82 (1999) 786.

[91] J.G. Darab, D.W. Matson, J. Electron. Mater. 27 (1998) 1068.

[92] A. Cabanas, J.A. Darr, E. Lester, M. Poliakoff, J. Mater. Chem. 11 (2001) 561.

[93] G. Vlaic, P. Fornasiero, S. Geremia, J. Kaspar, M. Graziani, J. Catal. 168 (1997) 386.

[94] G. Ranga Rao, J. Kaspar, R. Di Monte, S. Meriani, M. Graziani, Catal. Lett. 24 (1994) 107.

[95] P. Fornasiero, R. Di Monte, G. Ranga Rao, J. Kaspar, S. Meriani, A. Trovarelli, M. Graziani, J. Catal. 151 (1995) 168.

[96] N. Hickey, P. Fornasiero, J. Kaspar, M. Graziani, G. Blanco, S. Bernal, Chem. Commun. (2000) 357.

[97] M. Boaro, C. de Leitenburg, G. Dolcetti, A. Trovarelli, J. Catal. 193 (2000) 338.

[98] C. Janvier, M. Pijolat, F. Valdivieso, M. Soustelle, C. Zing, J. Eur. Ceram. Soc. 18 (1998) 1331.

[99] J.M. Kim, C.H. Shin, R. Ryoo, Catal. Today 38 (1997) 221.

[100] V.V. Srdic, M. Winterer, H. Hahn, J. Am. Ceram. Soc. 83 (2000) 1853.

[101] D. Terribile, A. Trovarelli, J. Llorca, C. de Leitenburg, G. Dolcetti, J. Catal. 178 (1998) 299.

[102] P. Trens, M.J. Hudson, R. Denoyel, J. Mater. Chem. 8 (1998) 2147.

[103] J.Y. Ying, C.P. Mehnert, M.S. Wong, Angew. Chem. Int. Ed. Engl. 38 (1999) 56.

[104] A.N. Shigapov, G.W. Graham, R.W. McCabe, H.K. Plummer, Appl. Catal. A Gen. 210 (2001) 287.

[105] G.W. Graham, H.W. Jen, R.W. McCabe, A.M. Straccia, L.P. Haack, Catal. Lett. 67 (2000) 99.

[106] G.W. Graham, H.W. Jen, W. Chun, R.W. McCabe, J. Catal. 182 (1999) 228.

[107] N. Izu, T. Omata, S. Otsuka-Yao-Matsuo, J. Alloys Compd. 270 (1998) 107.

[108] R.T. Baker, S. Bernal, G. Blanco, A.M. Cordon, J.M. Pintado, J.M. Rodriguez-Izquierdo, F. Fally, V. Perrichon, Chem. Commun. (1999) 149.

[109] P. Fornasiero, T. Montini, M. Graziani, J. Kaspar, A.B. Hungria, A. Martinez Arias, J.C. Conesa, Phys. Chem. Chem. Phys. 4 (2002) 149.

[110] J. Kaspar, R. Di Monte, P. Fornasiero, M. Graziani, H. Bradshaw, C. Norman, Top. Catal. 16 (2001) 83.

[111] M.H. Yao, R.J. Baird, F.W. Kunz, T.E. Hoost, J. Catal. 166 (1997) 67.

[112] T. Masui, K. Fujiwara, Y.M. Peng, K. Machida, G.Y. Adachi, Chem. Lett. (1997) 1285.

[113] R. Di Monte, J. Kaspar, P. Fornasiero, A. Ferrero, G. Gubitosa, M. Graziani, Stud. Surf. Sci. Catal. 116 (1998) 559.

[114] G. Centi, P. Fornasiero, M. Graziani, J. Kaspar, F. Vazzana, Top. Catal. 16 (2001) 173.

[115] R. Di Monte, P. Fornasiero, J. Kaspar, M. Graziani, J.M. Gatica, S. Bernal, A. Gomez Herrero, Chem. Commun. (2000) 2167.

[116] R. Di Monte, P. Fornasiero, J. Kaspar, M. Graziani, Stud. Surf. Sci. Catal. 140 (2001) 229.

[117] M. Fernandez-Garcia, A. Martinez-Arias, A. Iglesias-Juez, A.B. Hungria, J.A. Anderson, J.C. Conesa, J. Soria, Appl. Catal. B Environ. 31 (2001) 39.

[118] A. Martinez-Arias, M. Fernandez-Garcia, A. Iglesias-Juez, A.B. Hungria, J.A. Anderson, J.C. Conesa, J. Soria, Appl. Catal. B Environ. 31 (2001) 51.

[119] A. Martinez Arias, M. Fernandez Garcia, A.B. Hungria, J.C. Conesa, J. Soria, J. Alloys Compd. 323 (2001) 605.

[120] A. Martinez Arias, M. Fernandez Garcia, A.B. Hungria, A. Iglesias Juez, K. Duncan, R. Smith, J.A. Anderson, J.C. Conesa, J. Soria, J. Catal 204 (2001) 238.

[121] L.I. Podzorova, A.A. Ilicheva, N.A. Mikhailina, V.Y. Shevchenko, D.S. Bashlykov, G.V. Rodicheva, L.I. Shvorneva, Inorg. Mater. Engl. Tr. 37 (2001) 51.

[122] S. Rossignol, C. Kappenstein, Int. J. Inorg. Mater. 3 (2001) 51.

[123] H.C. Yao, Y.F. Yu Yao, J. Catal. 86 (1984) 254.

[124] J.Z. Shyu, W.H. Weber, H.S. Gandhi, J. Phys. Chem. 92 (1988) 4964.

[125] T. Miki, T. Ogawa, A. Ueno, S. Matsuura, M. Sato, Chem. Lett. (1988) 565.

[126] T. Horiuchi, Y. Teshima, T. Osaki, T. Sugiyama, K. Suzuki, T. Mori, Catal. Lett. 62 (1999) 107.

[127] M. Fernandez Garcia, A. Martinez Arias, A. Iglesias Juez, C. Belver, A.B. Hungria, J.C. Conesa, J. Soria, J. Catal. 194 (2000) 385.

[128] A. Piras, A. Trovarelli, G. Dolcetti, Appl. Catal. B Environ. 28 (2000) L77.

[129] J.Z. Shyu, K. Otto, J. Catal. 115 (1989) 16.

[130] A.J. Zarur, J.Y. Ying, Nature 403 (2000) 65.

[131] R.M. Heck, R.J. Farrauto, CATTECH 2 (1997) 117.